APPLYING ANN MODELING IN FATIGUE FAILURE OF GFRP

Raimundo Carlos Silverio Freire Júnior
UFRN – CT - Programa de Pós-Graduação de Engenharia Mecânica
Campus Universitário – Lagoa Nova –Natal – RN – CEP: 59072 - 970
E-mail: freirej@ufrnet.br

Eve Maria Freire de Aquino
UFRN – CT – Programa de Pós-Graduação de Engenharia Mecânica
Campus Universitário – Lagoa Nova –Natal – RN – CEP: 59072 - 970
E-mail: eve@dem.ufrn.br

Adrião Duarte Dória Neto
UFRN – CT – Programa de Pós-Graduação em Engenharia Elétrica
Campus Universitário – Lagoa Nova –Natal – RN – CEP: 59072 - 970
E-mail: adriao@dca.ufrn.br

Abstract. *The purpose of this paper is to assess the applicability of Artificial Neural Networks (**ANN**) and Adam's equation in the modeling of fatigue failure in polymer composites, more specifically in Glass Fiber Reinforced Plastic (GFRP). In the application of the model using **ANN** we show the feasibility of obtaining good results with a small number of S-N curves. The other model used involves applying empirical equations known as Adam's equations. A comparative study on the application of the aforementioned models is developed based on statistical tools such as correlation coefficient and mean square error. For this analysis we used composite materials in the form of laminar structures with distinct stacking sequences, which are applied industrially in the construction of large reservoirs. Reinforcements consist of mats and bidirectional textile fabric made of E-glass fibers soaked in unsaturated orthophthalic polyester resin. These were tested for six different stress ratios: **R** =1.43, 10, -1.57, -1, 0.1 and 0.7. The results showed that although **ANN** modeling is in the initial phase, it has great application potential.*

Keywords: *Artificial Neural Networks, Fatigue, Composites, Adam's Equations.*

1. INTRODUCTION

During a project involving structures and equipment submitted to cyclical loads in which composites are used as prime material, a large number of fatigue tests are often needed to obtain a certain level of confidence in the material. This is done mainly because little is known about the dynamic load response of these materials, thus making them unpredictable, as compared to conventional materials (Lee et al. 1999).

From the tests, we obtain the **S-N** curves (stress amplitude versus number of cycles) that are used in constructing Constant-Life Fatigue Diagrams, which are of great importance for the study and applicability of these materials. However, these diagrams, when built with a small number of **S-N** curves, underestimate or overestimate the current behavior of the composite, thus demonstrating the ever-increasing need to perform more tests for more accurate results (Philippidis, 2002).

Several studies (Subramanian et al., 1995; Philippidis et al., 2002; Wahl et al., 2002, Harris, 2003; Adam et al., 1989) have developed empirical models for fatigue behavior prevention of composite materials, related to both **S-N** curves and failure diagrams, such as Goodman's Diagram. These models have advantages and disadvantages in terms of applicability, and must be used considering statistical factors such as correlation coefficient (**r**).

The recent use of Artificial Neural Networks (**ANN**) for analyzing the fatigue behavior of composites (Vassilopoulos et al., 2007; El-Kadi et al., 2002; Al-Assaf et al. 2001) has proven the effectiveness of this technique, but the results obtained in the literature are still in their infant stage and much remains to be done.

The purpose of this paper is to model the fatigue behavior of two composite materials using Adam's equation and **ANN** architecture, compare the results and verify the feasibility of applying **ANN** in the analysis of fatigue behavior in composites. Furthermore, the error between the two models will be verified, considering a lower than conventional data set, where a data set with three and four **S-N** curves will be used to obtain the Constant-Life Fatigue Diagram curves.

We used two industrially manufactured composite laminates, made of orthophthalic polyester resin reinforced with E-glass fibers. Reinforcement is in the form of mats and bidirectional textile fabric. The mathematical modeling of these data was performed by first analyzing the **S-N** curves and then constructing a Goodman's Diagram using the equation proposed by Adam (Adam et al., 1989) and in the case of **ANNs** using the architecture proposed by the authors (Freire Jr. et al., 2005). In addition to fatigue tests, static uniaxial tensile and compression tests of the two laminates were also performed.

2. EXPERIMENTAL PROCEDURE

The laminates used in this study were industrially manufactured by the hand-lay-up process in the form of 1.0 m^2 plates. Unsaturated orthophthalic polyester resin was used as prime material and E-glass fiber reinforcement in the form of mats (5 cm, 450 g/m^2) and bidirectional textile fabric (450 g/m^2). Thus, two plates were manufactured, one with 10

and the other with 12 layers, thickness of 7.0 and 10.0 mm, respectively and with the following stacking sequences:

$$[M/T/M/T/M]_S \quad \textit{Stacking sequence of the } 10 \textit{ layer laminate } (C10)$$
$$[M/T/M/T/M/M/T/M/T/M/T/M] \quad \textit{Stacking sequence of the } 12 \textit{ layer laminate } (C12)$$

The symbols **M** and **F** refer to the mat and E-glass fiber bidirectional textile fabric, respectively. **C10** and **C12** refer to the 10 and 12-layer laminates, respectively. The symbol "**s"** refers to the symmetry of the material in relation to layer distribution; laminate **C10** is symmetrical whereas laminate **C12** is not.

Preliminary volumetric density and calcination tests were conducted on the two laminates to obtain the fiber volume percentage, which was 24.6% for the **C10** laminate and 24.9% for the **C12** laminate. It can be observed that the two laminates have roughly the same fiber percentages. Thus, it can be considered that any variation in mechanical properties occurring between them is only a result of a variation in their stacking sequence and the number of layers.

The plates were sectioned using a diamond cutter (DIFER D252), to avoid a possible "tearing away" of the fibers or any other type of damage to the test bodies. The dimensions of the test bodies for the uniaxial tensile test followed ASTM D 3039 (1990) norms, whereas those for uniaxial compression and fatigue were based on a study by Mandell et al. (1997). All the test bodies were rectangularly sectioned and in a predetermined laminate direction with the following dimensions: 200 x 25 mm for the uniaxial tensile and fatigue tests, and 100 x 25 mm for the uniaxial compression tests. The useful lengths (gauge) are 127 mm for the uniaxial tensile and fatigue test bodies with **R** – 0.1 and 0.7, 40 mm for the fatigue test bodies with **R** – 1.43, 10, -1.57 and -1 and 35 mm for the uniaxial compression test bodies. For each stress ratio the tests were conducted under constant amplitude stress, in which, 3 test bodies were used for each maximum load value chosen, for a total of 175 test bodies at the end of the testing. All the tests were conducted considering high cycle fatigue.

For the uniaxial tensile tests we used a Universal PAVITEST testing machine and for compression and fatigue tests we used an MTS-810. A displacement velocity of 1.0 mm/min was used in the tensile and compression tests and a frequency of 5 Hz in the fatigue tests. All the tests were conducted at ambient temperature (25 °C) with a relative air humidity of 50%.

The power law will be applied to obtain the **S-N** curves of the laminates under study and is presented in equation 1.

$$\log(\sigma_{max}) = A - B \cdot [\log(N)]^P \tag{1}$$

In the above equation, **A**, **B** and **P** are constants that must be obtained during the adjustment of the equations to the data, **N** is the number of failure cycles of the material and σ_{max} is the maximum cyclic stress component applied to the material. The values of constants **A**, **B** and **P** for each stress ratio given by equation 2 are shown in table 1, in which σ_{ultt} is the ultimate stress value and σ_{ultc} is the ultimate compression value. It should be pointed out that the calculation made to obtain these constants was for a 50% failure probability using the least squares method to arrive at these values.

Table 1. Constants obtained for equation 1 (power law) and the correlation coefficient (**r**) of each stress ratio for the two laminates studied (**C10** and **C12**).

R	**Laminate C10**			***r***	**Laminate C12**			***r***
	A	***B***	***P***		***A***	***B***	***P***	
1,43	2,23	0,00513	1,64	0,922	2,26	0,00458	2,04	0,972
10	2,23	0,00893	1,91	0,985	2,26	0,0255	1,57	0,994
-1,57	2,23	0,0407	1,35	0,991	2,26	0,0615	1,29	0,994
-1	2,06	0,0279	1,63	0,990	2,05	0,0330	1,68	0,993
0,1	2,06	0,00195	2,84	0,985	2,05	0,0163	1,78	0,991
0,7	2,21	0,0619	0,953	0,949	2,05	0,00512	2,12	0,966

For the modeling of Goodman's Diagram constant life curves, we used the equation proposed by Adam et al. (1989), presented in equation 2.

$$\frac{\sigma_a}{\sigma_{ultT}} = f \cdot \left(1 - \frac{\sigma_{med}}{\sigma_{ultT}}\right)^u \cdot \left(\frac{\sigma_{ultC}}{\sigma_{ultT}} + \frac{\sigma_{med}}{\sigma_{ultT}}\right)^v \tag{2}$$

In the above equation, $\boldsymbol{\sigma_a}$ represents the component of cyclical stress amplitude (maximum stress minus minimum stress divided by two); $\boldsymbol{\sigma_{med}}$ represents the component of mean cyclical stress (maximum stress plus minimum stress divided by two); $\boldsymbol{\sigma_{ultT}}$ is the ultimate stress value; $\boldsymbol{\sigma_{ultC}}$ is the ultimate compression value; **u**, **f** and **v** are the constants obtained during the adjustment of the curve to the data.

3. PROCEDURES FOR CREATING THE ANN MODEL

To create the mathematical model, we used the multiple-layer perception network trained by a backpropagation algorithm, with an architecture consisting of two input neurons (mean stress and number of cycles) and one output neuron (stress amplitude), in order to end up with a function that satisfied the condition shown in equation 3.

$$\sigma_a = f(\sigma_{med}, N) \tag{3}$$

In which $\boldsymbol{\sigma_a}$ is the stress amplitude applied (maximum stress minus minimum stress divided by two), $\boldsymbol{\sigma_{med}}$ is the mean stress (maximum stress plus minimum stress divided by two) and **N** is the number of cycles in which the material fractured.

We worked with a hidden layer with 2 to 30 neurons, all with bias and sigmoid activation function in the hidden neurons and linear function in the output neuron. The backpropagation training algorithm was used based on the momentum rule (Haykin, 2001).

Network training was based on **S-N** curve data, using equation 1. The power law has been used in studies by Philippidis et al., 2002, and Read et al., 1995.

A schematic diagram showing **ANN** training and the resulting **ANN** model is presented in figure 1. In this figure, **T** represents the number of functions (**S-N** curves obtained from equation 1) used for **ANN** training, **A** the number of functions used, **e** the error between the desired response and the current **ANN** response and **w** the matrix of synaptic weights of the **ANN.**

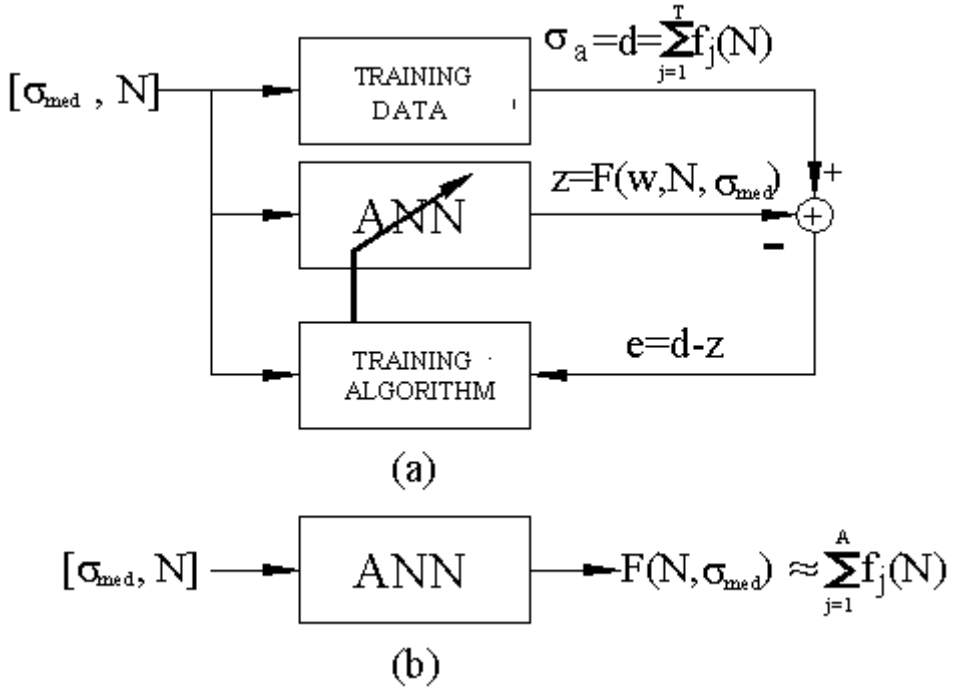

Figure 1. (a) **ANN** training method. (b) Model obtained from **ANN** training.

The values chosen for the current constant and the learning rate were 0.7 and 0.1, respectively. It is worth noting that these values are constant across all training epochs.

For **ANN** training we used two training sets, **3R** (R -10, -1.57 and 0.1), **4R (R** -10, -1.57, -1 and 0.1). These training sets were chosen to improve data distribution within the loading regions, using as criterion the number of test bodies used. During training we observed RMS (equation 4) behavior of the total data set in order to verify ANN generalization.

$$RMS = \frac{1}{(2 \cdot Q)} \cdot \sum_{1}^{Q} \sum_{i=1}^{m} (d_i - z_i)^2 \tag{4}$$

In the above equation **RMS** is the root mean square, **Q** represents the size of the data set, **m** the number of output neurons (for this study **m** = 1), $\mathbf{d_i}$ and $\mathbf{z_i}$ are the desired responses and the current response of the output knot, respectively.

The data are normalized both in the input neurons and output neuron; in the case of mean stress, normalization is done considering its signal (see figure 2). The purpose of this change in normalization was to achieve better data distribution and facilitate **ANN** learning (Haykin, 2001).

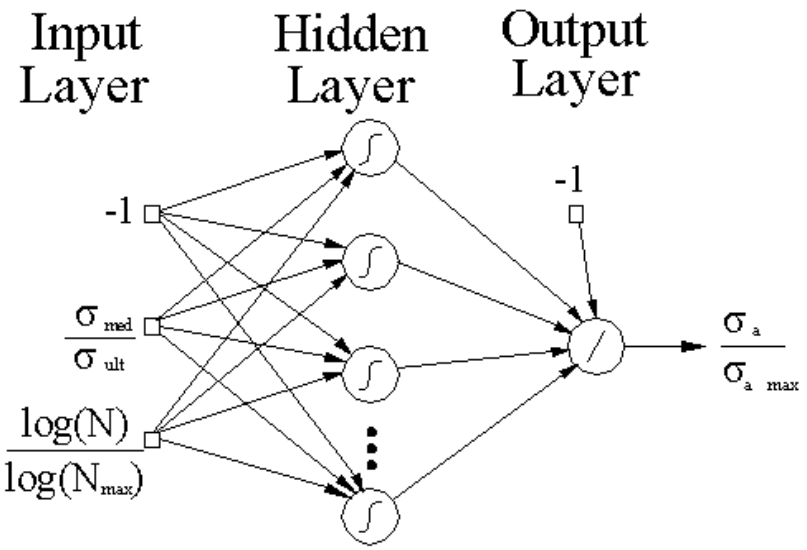

Figure 2. Diagram showing the **ANN** simulation model.

The range of analysis of the number of cycles in this study was between 10^2 and 10^7, given that the experimental data analyzed encompass this number of cycles. In addition to the data obtained from the **S-N** curves, we used the static test values in the training in order to facilitate **ANN** generalization.

The software used to implement all the algorithms used in this study was MATLAB.

4. RESULTS AND DISCUSSIONS

4.1. UNIAXIAL TENSILE AND COMPRESSION TESTS

Table 2 shows the results of the mechanical properties obtained in uniaxial tensile and compression tests for the two stacking sequences used. The results obtained for these two laminates are quite similar, for example ultimate stress, which is roughly 115 MPa for the two composite laminates. It is important to point out that the elastic moduli were measured in the direction of the applied load.

Given that the fiber percentages are practically the same, the introduction of 2 more layers (1 **M** and 1 **T**) did not cause great changes in the static mechanical response of the laminates.

*Table 2. Mechanical Properties of laminates **C10** and **C12**.*

	10 Layer Laminate	**12 Layer Laminate**
Modulus of Elasticity of Tensile (GPa)	4,81	4,50
Modulus of Elasticity of Compression (GPa)	4,27	4,79
Ultimate Stress of Tensile (MPa)	116,7	115,3
Ultimate Stress of Compression (MPa)	171,3	181
Maximum Strain of Tensile (%)	2,45	2,54
Maximum Strain of Compression (%)	4,07	3,92

4.2. FATIGUE TESTS: S-N CURVES

The **S-N** curves obtained for laminates **C10** and **C12** are represented in figures 3 and 4. The lowest normalized stress values were for **R** = -1 and **R** = -1.57. These results were expected, since for these cases the highest stress amplitudes in the laminate are applied as compared to the results of stress ratio for the same number of failure cycles. Similarly, the highest normalized stress values are found for **R** = 0.7 and **R** = 1.43, since the stress amplitudes applied for these stress ratios are very small as compared to the same number of failure cycles.

With respect to the graphs, it is important to note that the arrow symbol indicates that the test bodies were tested up to the number of cycles indicated, without fracturing. Furthermore, σ_{max} or σ_{min} and σ_{ultT} or σ_{ultC} were used in these graphs, depending on the type of stress ratio applied. That is, for **R** = 1.43 and **R** = 10, we used minimum stress (σ_{min}) and the ultimate stress of compression (σ_{ultC}), while for **R** = -1, **R** = -0.1 and **R** = 0.7, we used maximum stress (σ_{max}) and ultimate stress (σ_{ultT}). These variations were included in these graphs to enable a comparison of the results obtained for each stress ratio (**R**).

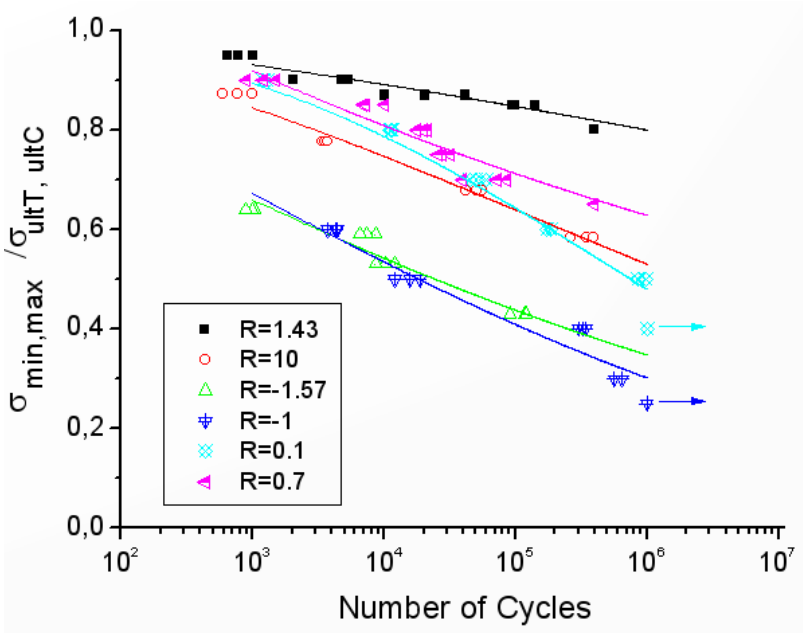

Figure 3. **S-N** curves of material **C10**, experimental data and model obtained by the power law.

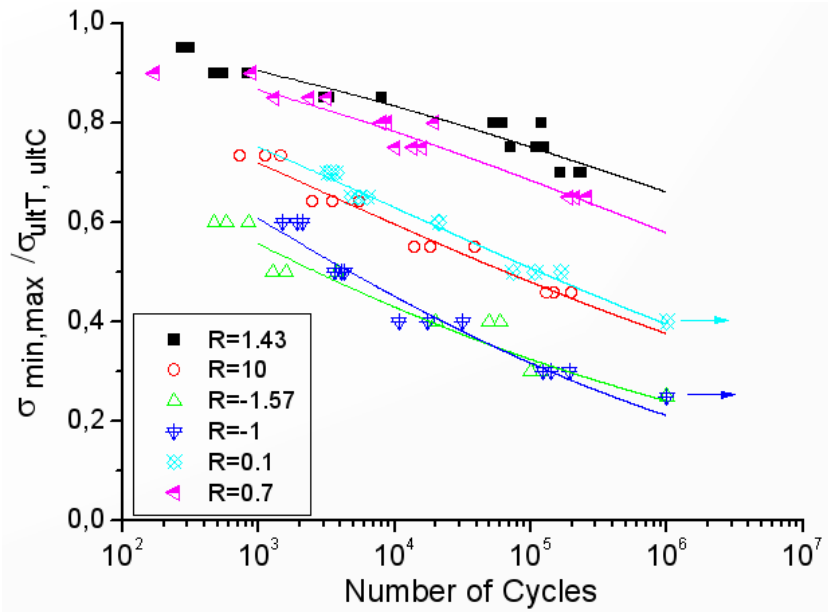

Figure 4. **S-N** curves of the material **C12**, experimental data and model obtained by the power law.

4.3. MODELING OF GOODMAN'S DIAGRAM FROM ADAM'S EQUATION

Goodman's Diagram was constructed from the results obtained by the **S-N** curves. The constant life curves were modeled by equation 2 for laminates **C10** and **C12.** These diagrams are shown in figures 4 and 5. Through these graphs one can see the importance of the tests for **R** = -1.57, since it was for this stress ratio that the highest stress amplitude values applied to the laminates were obtained for all the constant life curves analyzed, considering, of course, the same number of failure cycles. Thus, **R** = -1.57 has the largest safety region in terms of fatigue behavior of these materials. Because of this behavior, it can be affirmed that the two composite laminates have greater capacity to withstand variable cyclical loads (stress-compression) with a predominance of compression.

For **R** = 1.43, 0.1 and 0.7 in figures 4 and 5, it can be observed that the equation 2 curves approximate satisfactorily the results of the **S-N** curves (equation 1); however, there is a slightly more pronounced difference for the other stress ratios.

It is interesting to note that each constant life curve (for 10^3, 10^4, 10^5 and 10^6) of Goodman's Diagram shown in figures 4 and 5 are obtained using the results of the six **S-N** curves. If one wished to obtain the same findings using a lower number of results, they would likely be unsatisfactory. This is because each **S-N** curve represents only one point to be used to obtain constants for Adam's equation, for example, when there are only three **S-N** curves there will be only three points for obtaining each constant life curve, which would result in an unsatisfactory value.

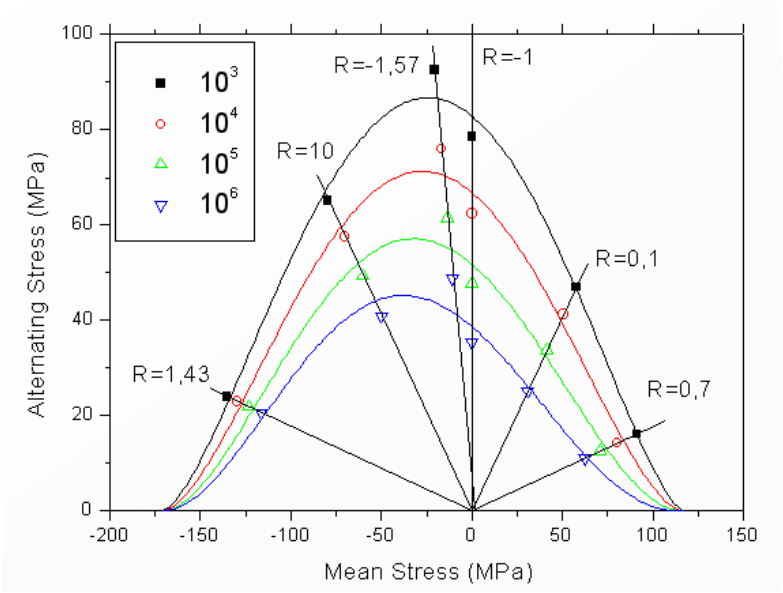

Figure 4. Goodman's Diagram modeled from Adam's equation, obtained for laminate **C10**.

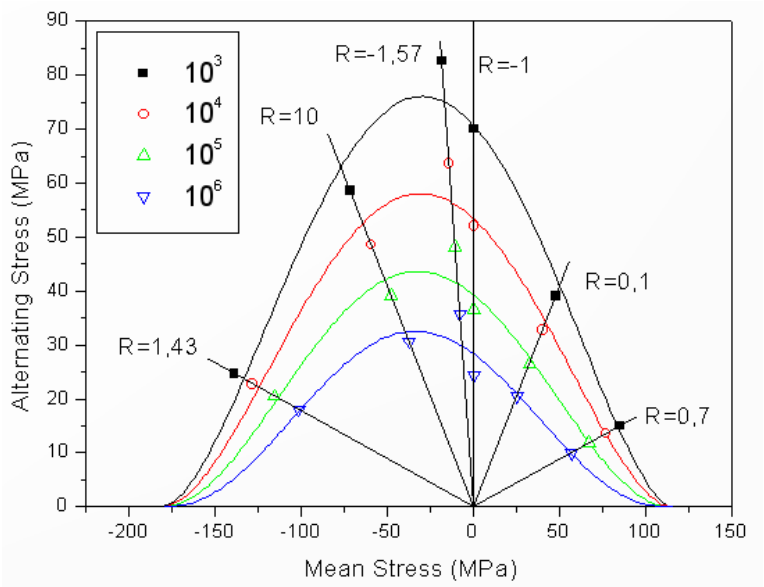

Figure 5. Goodman's Diagram from Adam's equation, obtained for **C12**.

Thus, in order to demonstrate quantitatively the importance of the number of **S-N** curves in mathematical modeling using Adam's equation, we verified the variation in the root mean square and in the correlation coefficient for the data sets applied in **ANN** training, which will be commented on in the next item, to obtain the constant life curves of Adam's model. The correlation coefficient (**r**) and root mean square ($\mathbf{RMS_{TOT}}$) for these data sets are shown in table 2.

Table 2. Correlation Coefficient and root mean square obtained when comparing between Adam's model data and those of **S-N** curves for each set used to obtain the constants.

Data Set	**Correlation Coefficient (r)**		**Root Mean Square ($\mathbf{RMS_{TOD}}$)**	
	C10	**C12**	**C10**	**C12**
3R	0,9771	0,6035	0,000939	0,0010
4R	0,9816	0,9787	0,000598	0,000633
Todos	0,9877	0,9853	0,000276	0,000253

hese results show that both the correlation coefficient and the root mean square achieve satisfactory results for at least 4 **S-N** curves. This problem exacerbates in some cases to the point of yielding totally unsatisfactory results, as can be observed for laminate **C12** modeled with set **3R,** where **r** is 0.6.

Thus, this empirical model presented by Adam does not have the capacity to predict results, contrary to what occurs with a well-trained **ANN**, as will be shown below.

4.4. MODELING OF GOODMAN'S DIAGRAM USING ANN's

From the training sets explained in item 3, we trained a three-layer neural network architecture using a technique known as cross validation.

This technique analyzes the RMS (root mean square) of the training set ($\mathbf{RMS_{TRA}}$) and of the total data set ($\mathbf{RMS_{TOT}}$) for each training epoch, so that at the end of training the synaptic weights of the network are chosen at the lowest value of $\mathbf{RMS_{TOT}}$.

The cross-validation results obtained during training showed that for all the training sets, the $\mathbf{RMS_{TOT}}$ and $\mathbf{RMS_{TRA}}$ curves displayed the following behavior: 1) the **RMS** curves follow one another, showing similar values; 2) the two curves separate after a determinate number of training epochs; at this point a minimum **RMS** value is obtained ($\mathbf{RMS_{MIN}}$), which is the lowest value obtained for the $\mathbf{RMS_{TOT}}$ curve during the entire training. After obtaining $\mathbf{RMS_{MIN}}$, the training set curve ($\mathbf{RMS_{TRA}}$) continues to fall while the total data set curve ($\mathbf{RMS_{TOT}}$) rises or stabilizes.

Figure 6 illustrates an example of $\mathbf{RMS_{TOT}}$ and $\mathbf{RMS_{TRA}}$ curves as a function of the number of training epochs analyzed.

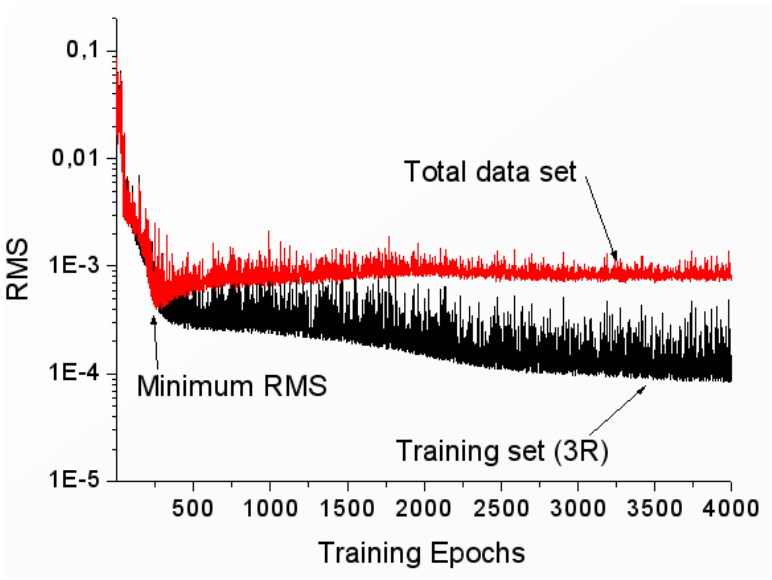

Figure 6. **RMS** curves obtained during ANN training with 27 hidden neurons and with training set **3R** for laminate **C12** (**R** -10, -1.57 and 0.1).

Table 3 shows the values for **RMS** and **r** (correlation coefficient) for the best results obtained for each training set. The results show that the increase in the number of **S-N** curves facilitates network learning, thus yielding results with a lower $\mathbf{RMS_{TOT}}$ value.

When comparing the results of table 3 with those obtained by Adam's equation (table 2) one can observe that the Neural Network yields more accurate results. For example, when $\mathbf{RMS_{TOT}}$ values obtained in **C10-4R** training are compared, it can be observed that the value obtained for Adam's equation is 0.0006 whereas for the Neural Network the value is 0.0003, a percentage variation of 50%.

Table 3. Best results obtained for each training set (the **ANNs** used between 2 and 30 hidden neurons and were trained up to 5000 epochs).

Composite Material	Training Set	Training Set		Total Data Set		Hidden Neurons	Training Epochs
		$\mathbf{EMQ_{TRE}}$	$\mathbf{r_{TRE}}$	$\mathbf{EMQ_{TOD}}$	$\mathbf{r_{TOD}}$		
C10	**3R**	0,00049	0,990	0,00048	0,987	23	287
	4R	0,00031	0,993	0,00030	0,992	9	1721
C12	**3R**	0,00037	0,989	0,00040	0,986	27	289
	4R	0,00027	0,992	0,00029	0,989	20	3577

From the Neural Networks trained with training sets **4R** presented in table 3, Goodman Diagrams were constructed for laminates **C10** (figure 7) and **C12** (figure 8).

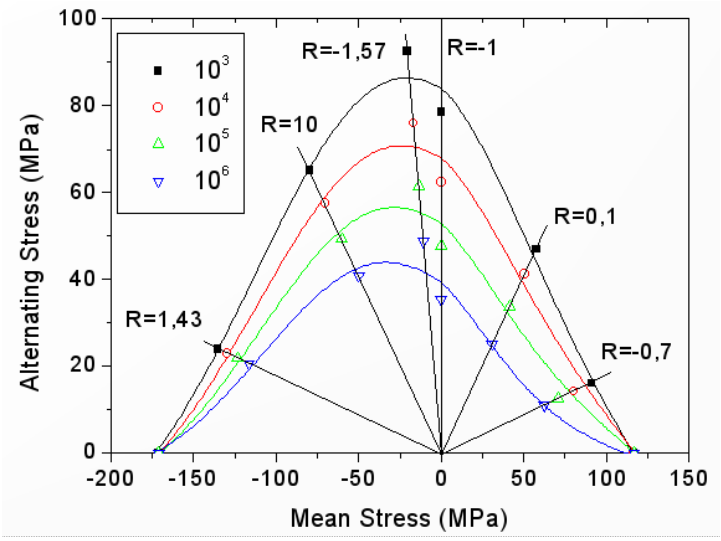

Figure 7. Goodman's Diagram obtained through the Neural Network with 9 hidden neurons trained with training set **4R** (**R** -10, -1.57, -1 and 0.1) for laminate **C10,** with 1720 training epochs.

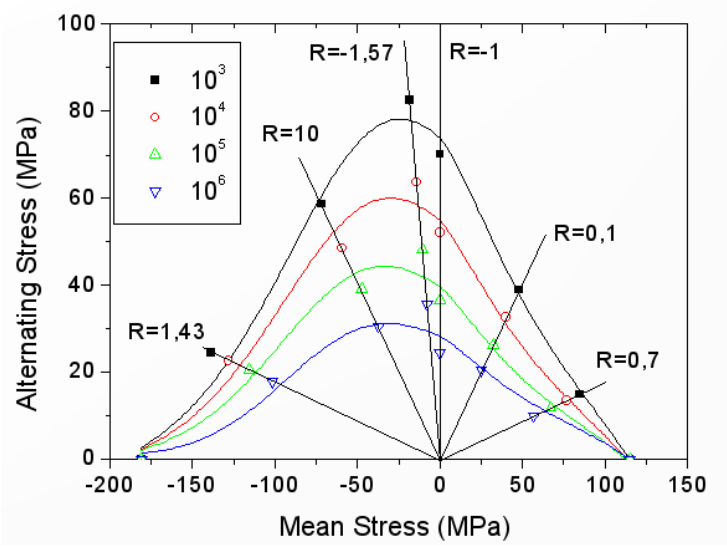

Figure 8. Goodman's Diagram obtained through the Neural Network with 20 hidden neurons trained with training set **4R** (**R** – 10, -1.57, -1 and 0.1) for laminate **C12**, with 3577 training epochs.

It can be observed in figures 7 and 8 that, much the same as the results obtained with Adam's equation (figures 4 and 5), there is a more pronounced difference in the curves for stress ratios 10, -1.57 and 0.1; however, in some of the constant life curves the error is less for the Neural Network than for Adam's equation.

It is always worth remembering that the Goodman Diagrams presented in Figures 7 and 8 were constructed using only 4 **S-N** curves in the Neural Network training. These results, together with data from other studies (Freire Jr et al., 2005) show the great potential of neural networks for analyzing fatigue behavior in composite materials, without forgetting that much more can still be done, given the innumerable types of training algorithms and architectures possible in neural network applications.

It must be emphasized that the pre-processing of data, using constants common to all composite materials, such as static constants (ultimate stress of tensile and of compression), makes this architecture and its training valid for any composite material, and according to the results, they model the fatigue behavior of these materials satisfactorily.

To compare the results of Adam's equation and those of the Neural Network, both obtained with 4 **S-N** curves, the graphs in figure 9 were drawn for laminate composites (a) **C10** and (b) **C12** (it is important to mention that the graphs in figure 9 and 10 were drawn considering only the maximum and minimum values of the constant life curves, that is, 10^3 and 10^6; this was done to facilitate the comparison of the results). These graphs show that, mainly for the constant life curves of 10^6 and for stress ratio region **R** = 1.43 and 0.7, Adam's equation did not produce good results. This behavior was expected, given that the data of these stress ratios were not used in the modeling. One can observe the benefit of Neural Network training, since satisfactory results were obtained using only 4 **S-N** curves not only for the data presented to the network but also for those not presented.

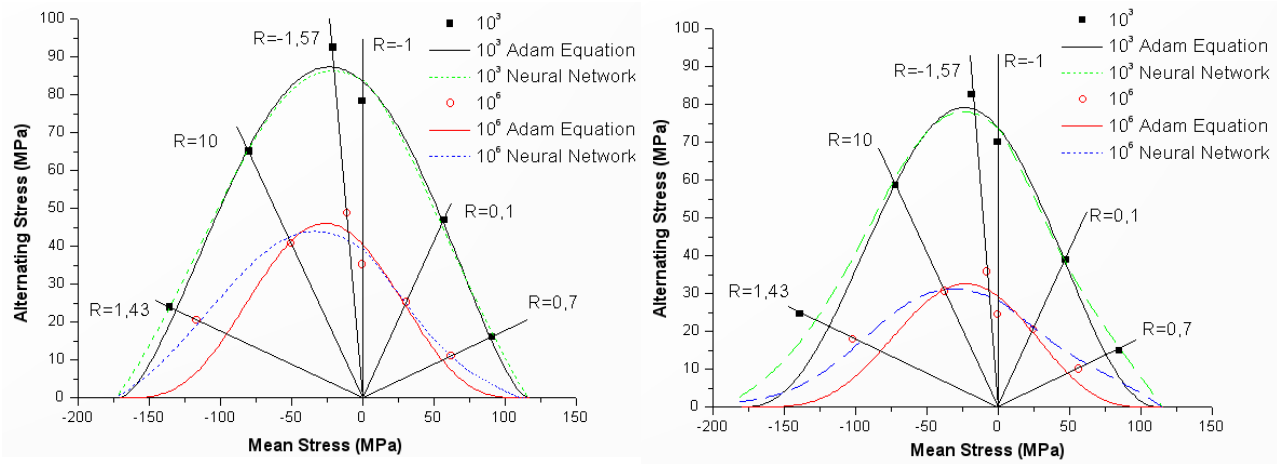

(a) (b)

Figure 9. Comparison of the modeling results obtained by Adam's equation (with 4 **S-N** curves) and by the Neural Network (with 4 **S-N** curves) for the constant life curves of 10^3 and 10^6 cycles, for laminates **C10** (a) and **C12** (b).

To compare the results obtained between Adam's equation and the Neural Network, we constructed the Goodman Diagrams shown in figure 10 for constant life curves of 10^3 and 10^6 cycles, using in this case all the **S-N** curves for the modeling of Adam' equation. The purpose of this new analysis was to verify which model was the most suitable for analyzing fatigue behavior in a qualitative manner.

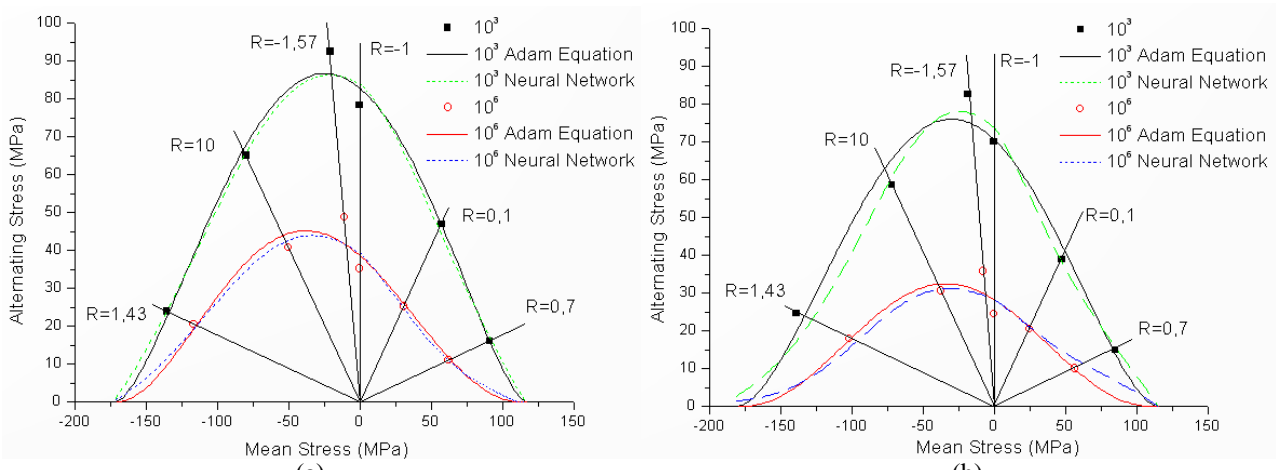

(a) (b)

Figure 10. Comparison of the modeling results obtained by Adam's equation (all the **S-N** curves) and by the Neural Network (4 **S-N** curves) for the constant life curves of 10^3 and 10^6 cycles, for laminates **C10** (a) and **C12** (b).

Figure 10 shows that there is a tendency, mainly for laminate **C12**, for the Neural Network model to yield better results for **R** =10 and -1.57 than Adam's model, always remembering that the Neural Network training only considered 4 **S-N** curves, whereas Adam's equation used all the results of the 6 **S-N** curves.

5. CONCLUSIONS

From the results obtained in static tests, it can be concluded that the stacking sequence of the material and the number of layers had little significant influence on most of mechanical properties, such as ultimate stress and modulus of elasticity measured in the load direction.

The results of fatigue tests show the importance of conducting tests for stress ratio **R** = -1.57, since the highest stress amplitudes applied in the two composite laminates were found here, with results compared for the same number of failure cycles, as shown in the Goodman Diagrams.

The modeling of Goodman's Diagram can be done using Adam's equation, but a large number of tests of **S-N** curves are required to ensure good representativity of fatigue failure. This does not occur for the Neural Network modeling of Goodman's Diagram. In this case excellent results were obtained for a much smaller universe of experimental data.

Neural network training proved to be the more efficient of the two models, given the need for fewer experimental data, that is, fewer tests, since more accurate results were obtained in preventing fatigue failure in the two composites..

6. ACKNOWLEDGEMENTS

The authors would like to thank CAPES (Coordination for Higher Level Graduates Improvement) for the research grant, the Mechanical Testing Laboratory at UFPB (Universidade Federal da Paraíba), Campus II for the use of MTS and to CEFET (Centro Federal de Educação Tecnológica) –RN for the use of PAVITEST.

7. REFERENCES

Adam, T., Fernando, G., Dickson, R. F., Reiter, H. and Harris, B., 1989, "Fatigue life prediction for hybrid composites", International Journal of Fatigue, Vol. 11(4), pp. 233-237.

Al-Assaf, y., El-Kadi, H., 2001, "Fatigue Life Prediction of Unidirectional Glass Fiber/Epoxy Composite Laminate Using Neural Network", Composite Structures, Vol. 53, No. 1, pp. 65-71.

ASTM D 3039, 1990, "Standard Test Method for Tensile Properties of Oriented Fiber Composites".

Beheshty, M. H., Harris, B. and Adam, T., 1999, "An Empirical Fatigue-Life Model for High-Performance Fibre Composites with and without Impact Damage", Composites – Part A: Applied Science and Manufacturing, Vol. 30, pp. 971-987.

El Kadi, H., Al-Assaf, Y., 2002, "Prediction of the Fatigue Life Prediction of Unidirectional Glass Fiber/Epoxy Composite Laminate Using Different Neural Network Paradigms", Composite Structures, Vol. 55, pp. 239-246.

Freire Jr., R. C. S., Doria Neto, A. D., Aquino, E. M. F., 2005, "Building of Constant Life Diagrams of Fatigue Using Artificial Neural Networks", International Journal of Fatigue, Vol. 27, pp. 746-751.

Harris, B., 2003, "A Parametric Constant Life Model for Prediction of the Fatigue Lives of Fibre Reinforced Plastics", Fatigue in Composite Materials, November, pp. 546-568.

Haykin, S., 2001, "Redes Neurais Princípios e Prática", 2° Ed., 893 p..

Herakovich, C. T., 1997, "Mechanics of Fibrous Composites", Ed. Elsevier, 460 p.

Lee, J. A., Almond, D. P., Harris, B., 1999, "The Use of Neural Network for the Prediction of Fatigue Lives of Composite Materials", Composites Part A: Applied Science and Manufacturing, Vol. 30, No. 10, pp. 1159-1169.

Mandell, J. F. and Samborsky, D. D., 1997, "DOE/MSU Composite Material Fatigue Database: test Methods, Materials and Analysis", SAND97-3002, Sandia National Laboratories, Albuquerque, 140 p.

Philippidis, T. P. and Vassilopoulos, A. P., 1999, "Fatigue of Composite Laminates under off-axis Loading", International Journal of Fatigue, Vol. 21, pp. 253-262.

Read, P., Shenoi, R., 1995, "A Review of Fatigue Damage Modelling in the Context of Marine FRP Laminates", Marine Structures, Vol. 8, pp. 257-278.

Subramanian, S., Reifsnider, K. L. and Stinchcomb, W. W., 1995, "A Cumulative Damage Model to Predict the Fatigue Life of Composite Laminates Including the Effect of a Fibre-Matrix Interphase", International Journal of Fatigue, Vol. 17, No. 5, pp. 343-251.

Sutherland, H. J., 1999, "On the Fatigue Analysis of Wind Turbines", SAND99-0089, Sandia National Laboratories, Albuquerque, 133 p.

Vassilopoulos, A. P., Georgopoulos, E. F., Dionisiopoulos, V., "Artificial Neural Networks in Spectrum Fatigue Life Prediction of Composite Materials", International Journal of Fatigue, Vol. 29, No. 1, pp. 20-29.

Wahl, N., Samborsky, D., Mandell, J. and Cairns, D., 2002, "Effects of Modeling Assumptions on the Accuracy of Spectrum Fatigue Lifetime Predictions for a Fiberglass Laminate", Wind Energy 2002, 19-26.